SMOOTH FACIES OF THE MAUNDER FORMATION AT ORIENTALE BASIN: EVIDENCES AND INTERPRETATIONS FOR COOLING BEHAVIOR OF MELT SHEET. J. Z. Ji[1,2], J. W. Head[2], L. Wilson[3], C. M. Pieters[2], J. Cassanelli[2], and J. Z. Liu[1]. [1]Institute of Geochemistry, CAS, Guiyang, China, [2]Brown University, Providence, USA, [3] Lancaster University, UK. (jinzju_ji@brown.edu).

Introduction: Impact melt deposits occur on the floors, walls and rims of lunar impact craters and basins. However, the nature of impact melt formation and evolution in lunar basins is uncertain. The Orientale basin [1-4] offers a unique opportunity to assess the nature of impact melt deposits and address questions concerning their volume, thickness, mode of emplacement, cooling and possible differentiation.

Maunder Formation: Lies inside the Outer Rook (OR) ring and consists of two facies[3-6]: 1) the outer corrugated or fractured facies, interpreted as being impact melt mixed with breccia clasts [1-3]; 2) the inner smooth plains facies, interpreted as a more pure impact melt [4, 5].

Melt Sheet: The prominent topography of the interior is composed of the IR plateau, and the inner depression, separated abruptly by the margin of the inner depression. Among the sources of immediate post-basin-collapse topography is general thermal equilibration of heat: 1) imparted to the substrate by the impact [7], of which impact melt is a significant part, and 2) caused by uplift of deep geotherms during collapse, both predicted to lead to thermal subsidence [7] because of cooling of the melt sheet with a maximum thickness of ~20-25 km [5].

Smooth Facies and Interpretation: We specifically describe and interpret four elements of the smooth facies of the Maunder Formation (Fig. 1):

1) Inner ring bounding scarp. Located at the edge of the inner ring depression along the western border, drops 2.8 km over a lateral distance of only ~12 km (Fig. 1a) and distinctly separates the fissured facies from the smooth facies of the basin interior. This scarp marks the location of the major thickness variation between the thin and more rapidly cooling Maunder fissured facies and the much thicker smooth facies of the more slowly cooling interior basin.

2) Marginal transitional deformed terrain. It is located between the steep scarp (Fig 1a) and the smooth plains with floor massifs (Fig. 1d,e) and represents a more transitional boundary between the fissured and smooth Maunder facies, with a 2.3 km high and ~30 km wide transition representing more of a draping of the melt sheet rather than a distinctive scarp (Fig. 1b). The smooth parts of the melt sheet are highly fractured with some parts separated by scarps of ~700 m relief. Portions of the melt sheet tilt toward the basin interior indicating preferential subsidence toward the melt sheet interior. These transitional deformed terrains manifest the more substantial central melt sea cooling by faulting, fracturing and tilting of the margins of the cooling and thickening melt boundary layer.

3) Hummocky floor topography. This hummocky texture (Fig. 1c) is composed of small mounds and hummocks, short linear ridges and fissured troughs. Topographic relief is typically 100-200 m, but can be locally up to ~500 m. We tentatively interpret this terrain as remnants of a quenched crust that contained floating elements of impact breccia fragments.

4) Floor massifs. These features consist of central mountains rising hundreds of meters above a relatively flat irregularly shaped plateau (Fig. 1d,e), 10-20 km widths, with 300-500 m steep marginal scarps. These features are interpreted as “rockbergs” in which km-scale excavated crustal fragments float in the impact melt sea, cool their surroundings, and then fracture at the edge of the cooled plateau as the adjacent hotter melt continues to solidify and subside.

Conclusions: These observations and stratigraphic relationships help to confirm an impact melt origin for the Maunder Formation and provide initial quantitative data on the cooling history of the Orientale melt sheet.

References: [1] Head J. W. (1974) The Moon 11, 327. [2] Howard et al. (1974) RGSP 12, 39. [3] McCauley (1977) PEPI 15, 220. [4] Whitten et al. (2010) LPSC XLI #1841. [5] Wilson & Head (2011) LPSC XLII #1345. [6] Head & Wilson (1992) G&CA 56, 2155. [7] Bratt et al. (1985) JGR 90, 12,415. [8] Barker et al. (2016) Icarus, 273.

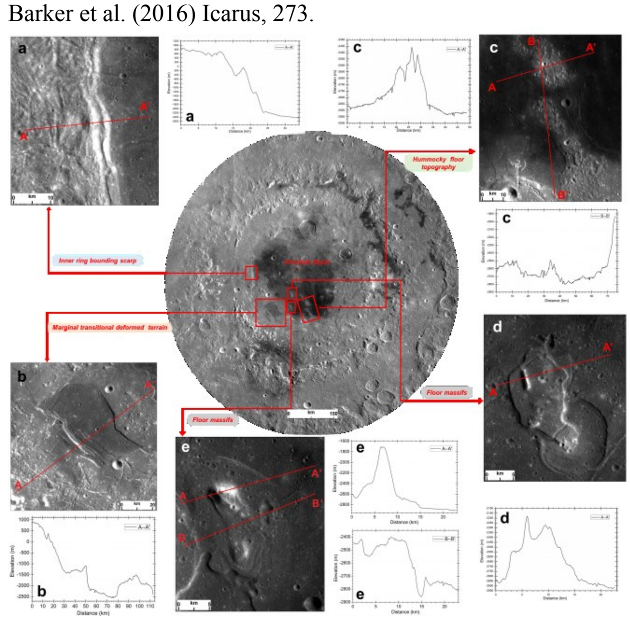

Figure 1. Surface structure and topography of Orientale Maunder Formation (Kaguya TC image and SLDEM2015 [8])